

## 200-fold lifetime extension of 2,6-dihydroxyanthraquinone during flow battery operation

Meisam Bahari<sup>1,2</sup>, Yan Jing<sup>3</sup>, Shijian Jin<sup>1</sup>, Marc-Antoni Goulet<sup>1,4</sup>, Tatsuhiro Tsukamoto<sup>3</sup>, Roy G Gordon<sup>3</sup>, Michael J Aziz<sup>1</sup>

<sup>1</sup>John A. Paulson School of Engineering and Applied Sciences, Harvard University, Cambridge, MA, USA

<sup>2</sup>Present address: Quino Energy, Inc., 2235 Polvorosa Ave., Ste. 230, San Leandro, CA, USA

<sup>3</sup>Department of Chemistry and Chemical Biology, Harvard University, Cambridge, MA, USA

<sup>4</sup>Present address: Department of Chemical and Materials Engineering, Concordia University, Montreal, Quebec, Canada

### Abstract:

We study the capacity fade rate of a flow battery utilizing 2,6-dihydroxyanthraquinone (DHAQ) and its dependence on hydroxide concentration, state of charge, cutoff voltages for the discharge step and for the electrochemical regeneration (oxidation of decomposition compounds back to active species) step, and period of performing the electrochemical regeneration events. Our observations confirm that the first decomposition product, 2,6-dihydroxyanthrone (DHA), is stable but after electro-oxidative dimerization, the anthrone dimer decomposes. We identify conditions for which there is little time after dimerization until the dimer is rapidly re-oxidized electrochemically to form DHAQ. Combining these approaches, we decrease the fade rate to 0.02%/day, which is 18 times lower than lowest rate reported previously of 0.38%/day, and over 200 times lower than the value under standard cycling conditions of 4.3%/day. The findings and their mechanistic interpretation are expected to extend the lifetime and enhance the effectiveness of *in-situ* electrochemical regeneration for other electroactive species with finite lifetimes.

### Introduction:

Although the cost of emissions-free electricity from photovoltaics and wind power has dropped below the cost of fossil fuel-generated electricity, the intermittency of these renewable resources presents an increasingly difficult problem as their contribution to the generation mix grows.<sup>1</sup> One potential solution is storing energy from these sources when available and then utilizing it when necessary. In addition to utilizing renewable sources, stationary storage also plays a significant role in balancing the power supply and demand for grid electricity.<sup>2</sup>

Various energy storage systems have been developed so far, amongst which flow batteries are particularly suitable for grid storage needs.<sup>3</sup> The unique architecture of flow batteries makes it possible to decouple power and energy scaling, offering system flexibility to fit a wide range of specifications for power and discharge duration, i.e. energy/power ratio. Aqueous flow batteries, in particular, utilize water as the solvent and have no flammability concern.<sup>4</sup> Operating in water also brings a significant cost advantage. Aqueous-soluble organic energy-storing molecules, benefiting from structural diversity and the earth-abundance of their atomic components, may permit scalable, safe, cost-effective long duration energy storage in aqueous redox flow batteries.<sup>5-7</sup>

From the cost perspective, one of the promising energy-storage molecular families is that of anthraquinone derivatives<sup>8-11</sup>, such as 2,6-dihydroxyanthraquinone (DHAQ<sup>2-</sup> or DHAQ for simplicity)<sup>12</sup>, whose cost is low at a mass production scale (~\$4/kg).<sup>13</sup> However, the main challenge of utilizing DHAQ as the negolyte (negative electrolyte) species is its fast decomposition rate caused by the instability of reduced DHAQ (DHAQ<sup>4-</sup>). The decomposition mechanism of DHAQ<sup>4-</sup> has been identified, and two

strategies for reducing and reversing this decomposition have been demonstrated.<sup>14-16</sup> The first strategy involves restricting the state of charge (SOC) of the negolyte.<sup>14</sup> The second approach is to electrochemically oxidize the decomposition product, 2,6-dihydroxyanthrone (DHA), back into DHAQ.<sup>16</sup> The latter approach involves lowering the cell voltage during the discharge step to values where the negolyte, specifically the decomposition products, experiences a more positive potential than in normal cycling. As a result, the side products are oxidized back to DHAQ.

A flow battery utilizing DHAQ exhibits a temporal fade rate of ~4.3%/day (measured in this study) under normal cycling conditions. When the electrochemical regeneration strategy is implemented, a fade rate of 0.38%/day is reported, which is over an order of magnitude improvement.<sup>16</sup> However, this fade rate is still very fast, preventing DHAQ from being an attractive negolyte species for commercialization purposes despite its low predicted cost of manufacture. This study aims to explore the possibility of further reducing the fade rate. Thus, the effects of various factors that may affect the effectiveness of the electrochemical regeneration technique and the fade rate are investigated. These factors are the concentration of OH<sup>-</sup>, the cutoff voltage of the discharge step in normal cycling, the cutoff voltage of the regeneration step, and the period of the periodic regeneration events. Properly controlling these factors combined with restricting the negolyte SOC to 0-85% leads to a fade rate as low as 0.02%/day, which is over 200 times lower than that under standard cycling conditions. The findings and mechanistic insights obtained in this study are anticipated to improve the effectiveness of *in-situ* electrochemical regeneration for other electroactive species with finite lifetimes.

## Results and discussion

### pH effect

The impact of pH on the fade rate has been reported before.<sup>17</sup> However, hydroxide concentrations higher than 1.0 M have rarely been examined. Figure 1a shows the time-dependence of the discharge capacity of a cell that contains 0.1 M DHAQ in the negolyte and 0.06M/0.03 M ferrocyanide/ferricyanide in the posolyte in 1.0 M OH<sup>-</sup>. Similar tests were performed at various OH<sup>-</sup> concentrations and the fade rates are shown on Figure 1b (for the definition of fade rate refer to the SI). Increasing the OH<sup>-</sup> concentration over the range 0.1–2.0 M reduces the fade rate from ~100%/day to only ~0.4%/day in 2.0 M OH<sup>-</sup>. Interestingly, the fade rate in 2.0 M OH<sup>-</sup> is very close to the fade rate of 0.38%/day previously reported in 1.0 M OH<sup>-</sup> when the electrochemical regeneration technique was implemented.<sup>16</sup> Clearly, raising the concentration of OH<sup>-</sup> beyond 1.0 M can noticeably reduce the fade rate.

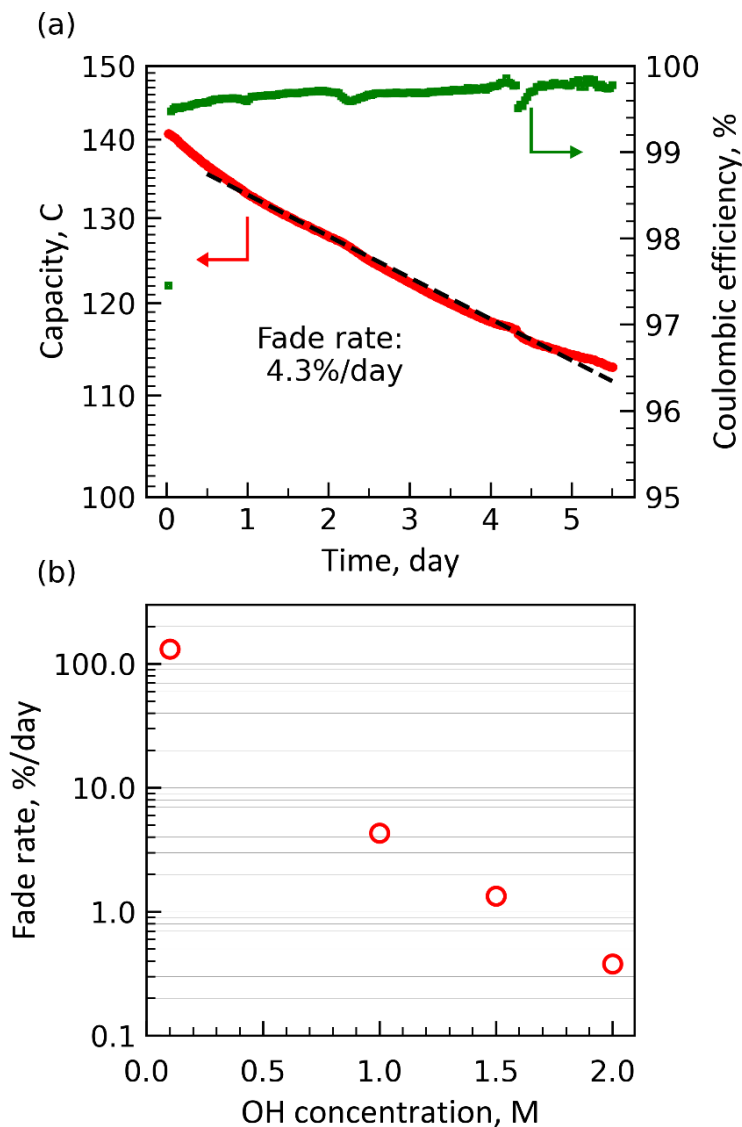
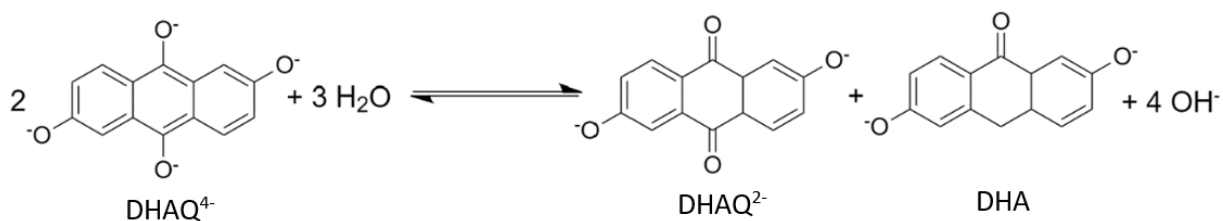


Figure 1: (a) Semi-log plot of discharge capacity and coulombic efficiency vs. time for a DHAQ | ferro/ferricyanide full cell in 1 M OH<sup>-</sup>, (b) Fade rate as a function of OH<sup>-</sup> concentration. Test conditions: negolyte contained 5.5 ml of 0.1 M DHAQ, and the posolyte consisted of 30 ml of 0.06 M potassium ferrocyanide and 0.03 M potassium ferricyanide. Cycling was performed under constant current density at 50 mA/cm<sup>2</sup> followed by a potentiostatic hold. Cutoff voltages for the charge and discharge steps were 1.4 and 0.9 V, respectively. Cutoff current densities for the charge and discharge steps were 2 and 1 mA/cm<sup>2</sup>, respectively.

The effect of OH<sup>-</sup> concentration on the fade rate can be understood by considering the disproportionation reaction of DHAQ<sup>4+</sup>. As shown in Scheme 1, 4 moles of OH<sup>-</sup> are formed when two moles of DHAQ<sup>4+</sup> disproportionate. At elevated OH<sup>-</sup> concentration, the equilibrium shifts to the left, favoring DHAQ<sup>4+</sup> over the formation of DHA.



Scheme 1: Disproportionation reaction of  $\text{DHAQ}^{4-}$  <sup>14, 17</sup>

### Electrochemical regeneration

To achieve a low fade rate, the electrochemical regeneration technique was integrated into the cell cycling in 2.0 M  $\text{OH}^-$ . Because the fade rate in 2.0 M  $\text{OH}^-$  is reasonably low ( $\sim 0.4\%$ /day), we hypothesized that, combined with the effect of regeneration, the fade rate should be lowered dramatically. As shown and annotated on Figure S2, however, the regeneration in 2.0 M  $\text{OH}^-$  is noticeably less effective and unpredictable in contrast to the value of 90% previously reported for 1.0 M  $\text{OH}^-$ <sup>16</sup>. Interestingly, when the discharge cutoff voltage was raised to 0.95 V or higher, the recovery efficiency, defined as the fraction of the electroactive species lost since the previous regeneration step that is converted back into electroactive species during the regeneration step, became repeatable and remained at 88%. The effectiveness of the regeneration step thus appears to be very sensitive to the cycling discharge cutoff voltage.

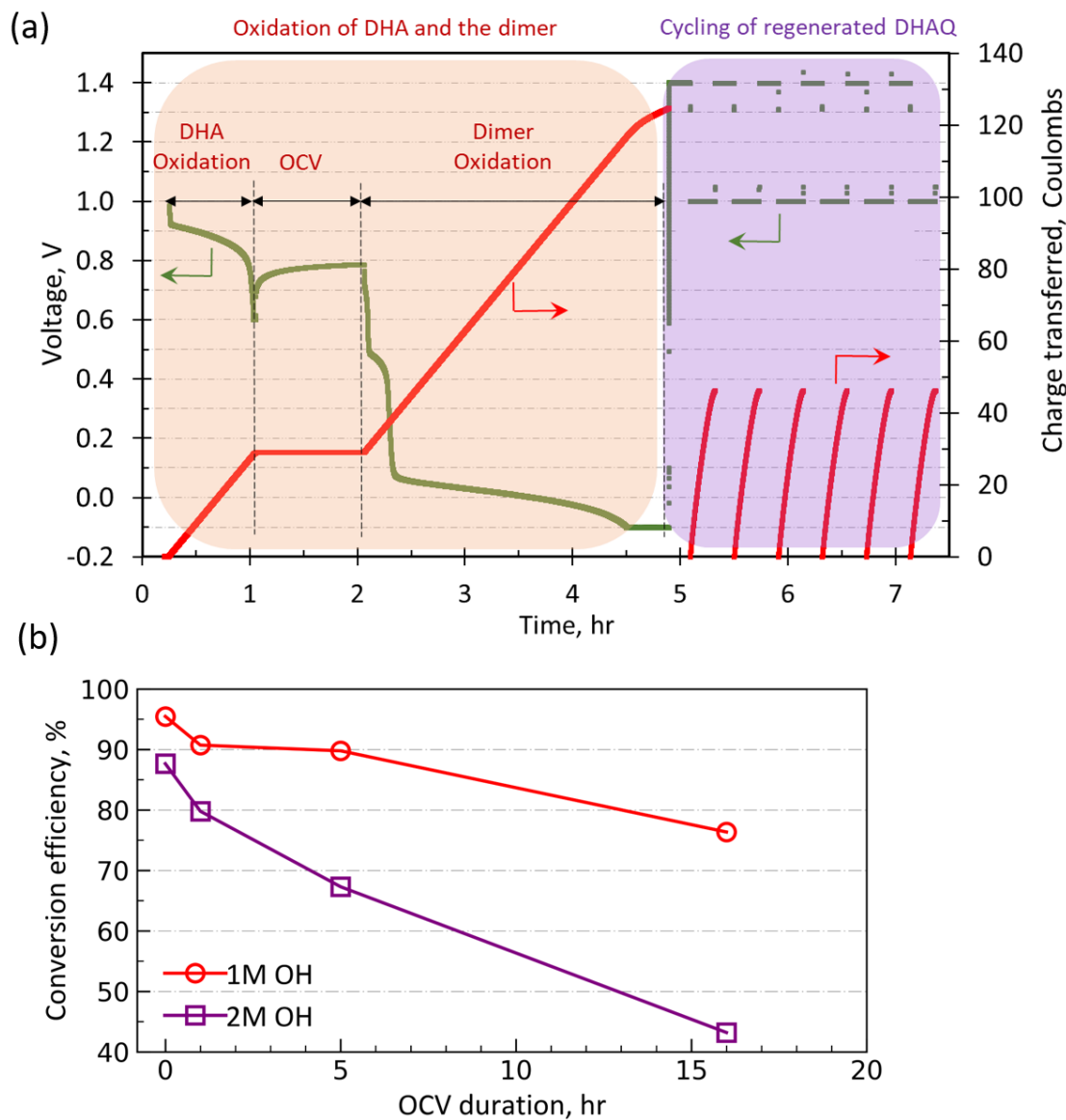


Figure 2: Conversion of DHA to DHAQ. a) Time-dependence of voltage and charge transferred in a DHA | ferro/ferricyanide full cell in 2 M OH<sup>-</sup>. b) conversion efficiency vs. OCV duration. Test conditions: negolyte contained 6.5-7.0 ml of 0.05 M DHA, and the posolyte comprised 120 ml of 0.04 M potassium ferrocyanide and 0.02 M potassium ferricyanide. DHA oxidation conditions: constant current density at 2 mA/cm<sup>2</sup> followed by potentiostatic hold at 0.6 V until a cutoff current density of 0.75 mA/cm<sup>2</sup> was reached. Dimer oxidation conditions: constant current density at 2 mA/cm<sup>2</sup> followed by potentiostatic hold at -0.1 V until a cutoff current density of 0.75 mA/cm<sup>2</sup> was reached. Cycling of the formed DHAQ: constant current density of 50 mA/cm<sup>2</sup> followed by a potentiostatic hold. The cutoff voltage for the charge and discharge steps were 1.4 V and 1.0 V, respectively. Cutoff current densities for the charge and discharge steps were 2 mA/cm<sup>2</sup>.

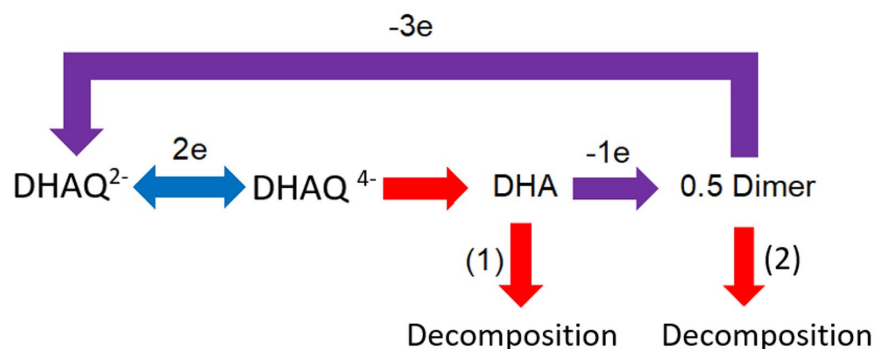
### Stability of DHA and the dimer

To understand the observations described above, we investigated how DHA, the disproportionation product of DHAQ<sup>4-</sup>, is affected under various cycling conditions in the negolyte against a ferro/ferricyanide posolyte. We define the conversion efficiency as the fraction of DHA converted to DHAQ. Because the main decomposition product in a DHAQ | ferro/ferricyanide cell is DHA<sup>14</sup>, the conversion efficiency is

expected to remain the primary determinant of the recovery efficiency. However, other decomposition mechanisms, implications of which are not entirely discerned, may also contribute to the recovery efficiency.

In Figure 2a we show the cell voltage vs. time starting with 100% DHA at  $t=0$ . DHA oxidation commences at approximately 0.2 hr and ends at 1.0 hr. Next, the cell is held at open-circuit for the second hour, and then put through another negolyte oxidation step at a very low cell voltage (-0.1V) during hours 2-5. Finally, the last three hours are devoted to cycling with voltage and current cutoff values appropriate for DHAQ, to evaluate the discharge capacity attributable to the DHAQ formed from DHA. The amount of DHAQ, reckoned from the accessed discharge capacity, is compared to the theoretical amount that may possibly form from the initial DHA, and their ratio reported in Figure 2b.

Examination of the voltage profile during the oxidation of DHA reveals that this compound turns into the DHA dimer at a quite high cell voltage, around 0.9 V. Thus, if the discharge cutoff voltage of a DHAQ | ferro/ferricyanide cell is set at or below this value, then DHA, which forms gradually due to the disproportionation of  $\text{DHAQ}^{4-}$  (Scheme 1), may get electrochemically oxidized to the dimer even during regular cycling. Consequently, a mixture of DHA and dimer exists in the negolyte well before the onset of a regeneration step. Thus, we hypothesized that the inefficiency of the regeneration procedures at discharge cutoff voltages of 0.9 V or lower in Figure S2 is related to the gradual decomposition of DHA, the dimer, or both, exacerbated at higher  $\text{OH}^-$  concentrations. The hypothesized decomposition reactions starting from DHA and the dimer are shown by red arrows and labeled as either (1) or (2) in Scheme 2 and are assumed to be homogeneous chemical reactions. Disproportionation reaction of  $\text{DHAQ}^{4-}$  to DHA is also shown by a red arrow. Note this scheme does not intend to show an exhaustive reaction pathway.



Scheme 2: Reactions considered in a DHAQ negolyte. Blue arrow: electrochemical reactions during regular cycling; red arrows: decomposition reactions; purple arrows: electrochemical reactions for the regeneration of DHAQ from DHA. Red arrows labeled as either (1) or (2) are decomposition reactions hypothesized in this work, and the rest are adapted from Ref. <sup>14</sup>.

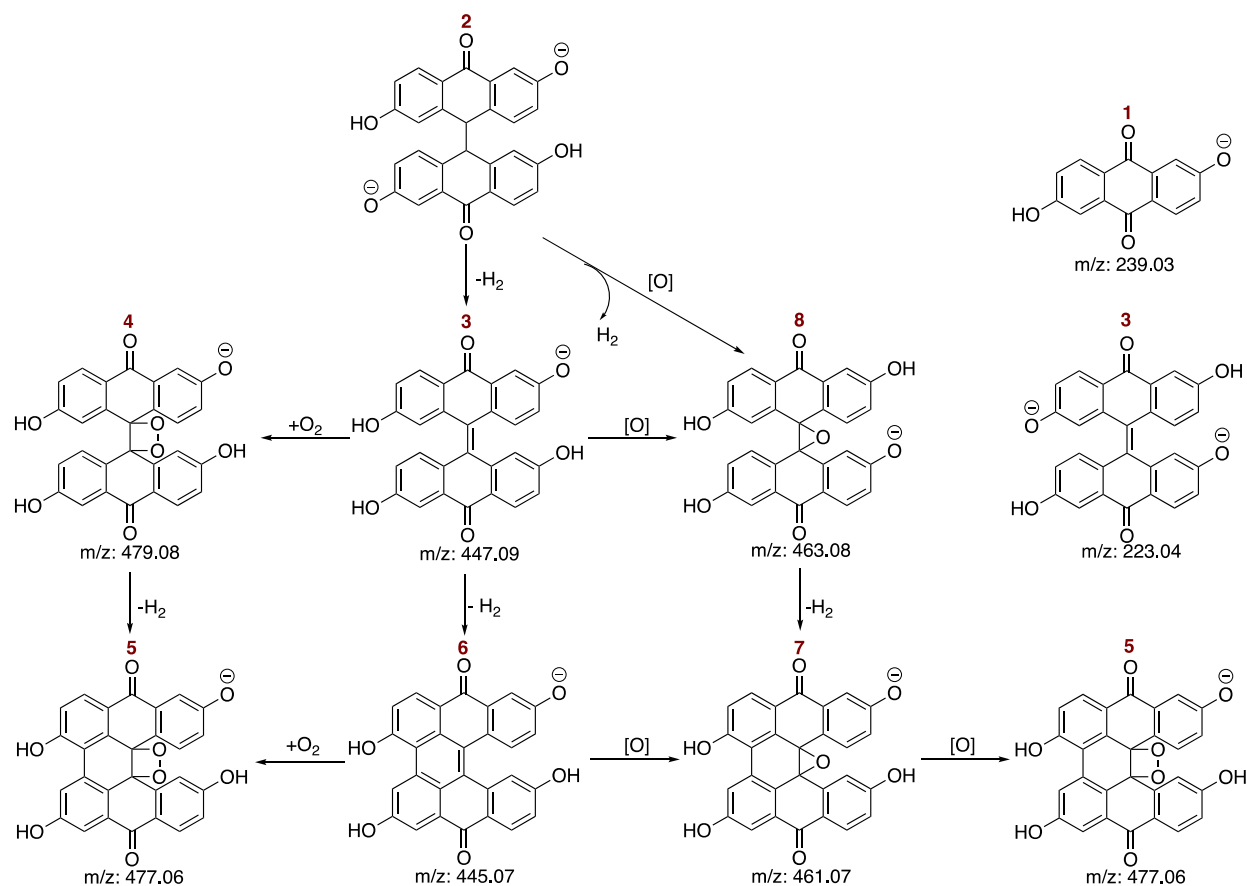
To test the hypothesis, experiments were performed using chemically synthesized DHA instead of analyzing the DHA that gradually accumulates through cycling of DHAQ. The latter process is very slow, especially in 2.0 M  $\text{OH}^-$  where the fade rate is only  $\sim 0.4\%$ /day (Figure 1). The same amount of DHAQ was generated by electrochemical oxidation of a freshly made DHA electrolyte and of an otherwise-identical electrolyte that sat for more than four weeks under an inert nitrogen atmosphere. This observation indicates that DHA itself is chemically stable and does not undergo any chemical decomposition. Therefore, the red arrow labeled as (1) represents a reaction that either does not occur or occurs at a negligible rate.

To test the possibility of the chemical decomposition of the dimer, i.e., the reaction (2) in Scheme 2, DHA is oxidized to the dimer, but the electrochemical oxidation of the dimer is delayed for a certain

amount of time, referred to as 'OCV duration', during which the cell is kept under OCV, to evaluate the extent of dimer decomposition under OCV conditions. Figure 2a shows a sample plot of voltage and charge transferred of a test with only one hour of OCV duration. Tests were performed with various OCV duration. The electrochemical oxidation of the remaining dimer is then initiated with a deep discharge.

As shown in Figure 2b, a longer OCV duration leads to less formation of DHAQ from the dimer. Whereas over 95% of DHA is converted to DHAQ with a zero OCV duration, the conversion efficiency drops to 76% with 16 hours of OCV duration. This adverse effect is more pronounced at elevated  $\text{OH}^-$  concentration, where the conversion efficiency drops to 43% with 16 hours of OCV duration. This suggests that the dimer decomposes more rapidly with increasing  $\text{OH}^-$  concentration. To minimize its decomposition, the dimer should be converted to DHAQ as soon as the dimer forms. Figure 2b also shows that even with zero OCV duration, the conversion of DHA to DHAQ is incomplete and lower in 2.0 M  $\text{OH}^-$  than in 1.0 M  $\text{OH}^-$ . This observation suggests that the decomposition of dimer can be limited but not entirely prevented because of its fast decomposition rate. Note that we cannot exclude the possibility of other decomposition reactions that may occur during the oxidation of DHA. However, no decomposition products were observed using NMR. In Figure 2a, another electrochemical reaction takes place at around 0.45 V; however, the origin of the reaction is still unclear.

In order to investigate side products that may form during the conversion of DHA to DHAQ, a DHA negolyte was oxidized and species in the negolyte were tracked during the conversion via LC-MS. The results are presented in Figure S4 and indicate that the dimer is oxidized by homogeneous chemical reaction(s) even when it is left under OCV. In addition to the formation of DHAQ ( $m/z = 239.03$ ), other previously unexplored species that have  $m/z = 461.07$ , 463.08, and 477.08 also grow. Based on Figure S4b, the subsequent electrochemical oxidation process enables the formation of DHAQ from the decomposed species. Nevertheless, the residual species ( $m/z = 463.08$  and 479.08) imply that the regeneration process fails to convert all the dimer to DHAQ; in other words, the DHA dimer is irreversibly decomposed to these species, leading to a permanent capacity loss.



Scheme 3: Proposed molecular structures with  $m/z$  values found by LC–MS analysis and the hypothesized DHA dimer decomposition pathways.

Scheme 3 depicts proposed molecular structures with  $m/z$  values found by LC-MS analysis and the hypothesized DHA dimer chemical decomposition pathways. The high concentration of hydroxide ions facilitates the deprotonation of methine groups in the (DHA)<sub>2</sub> (**2**), thus driving the electrochemical desaturation to produce **3**, which may be related to the voltage plateau starting at 0.4 V in Figure 2a. **3** can be oxygenated to form **4** and **8**. The compounds **3**, **4**, **8** can undergo dehydrogenative cyclization reactions to produce **6**, **5**, **7**, respectively; corresponding  $m/z$  values have been detected from the LC–MS experiments. However, it is still unclear whether **4–8** were generated during the oxidation process in electrochemical flow cells then detected by the LC–MS experiments or produced under LC–MS experiment conditions in the presence of oxygen, as **4–8** were mainly observed in Samples 1 and 2. For Sample 3, the intensity of **1** increased whereas the intensity of **4**, **7**, and **8** dropped. Nevertheless, we cannot rule out that **4–8** were further electrochemically oxidized to form polyfused aromatic species that became aqueous-insoluble and precipitated on electrodes or other cell parts, thus less likely to be detected through LC–MS experiments. Further mechanistic insight needs additional study.

With the insights gained on the decomposition of dimer, we can now explain our earlier observation where lowering the discharge cutoff potential down to 0.3 V adversely affects the DHAQ recovery efficiency (Figure S2). Conversion of DHA to DHAQ includes two electrochemical oxidation reactions as depicted in Scheme 2: DHA  $\rightarrow$  0.5 Dimer and then 0.5 Dimer  $\rightarrow$  DHAQ. Between these two, the first reaction proceeds at a higher cell voltage (e.g. a less positive oxidation potential for the negolyte) than the second: as shown in Figure 2a, the first and second reactions are initiated at cell voltages of about 0.9 V and 0.0 V, respectively, and proceed to completion as the cell voltage is lowered further, increasing the

driving force for the reactions. Lowering the cycling discharge cutoff voltage to 0.3 V not only oxidizes the DHAQ<sup>4-</sup> (reduced form of DHAQ), but it also oxidizes any DHA formed during the disproportionation reaction to the dimer. Nevertheless, the cell voltage is not low enough to proceed to the oxidation of the dimer; this causes the accumulation of dimer, which is unstable, in the electrolyte. The dimer undergoes a decomposition reaction until the cell voltage is lowered enough during the deep-discharge step to oxidize the remaining dimer.

Therefore, we conclude that the cell discharge cutoff voltage should be set high enough (0.95 V or higher for the conditions tested in this study) to prevent the oxidation of DHA to the dimer. Otherwise, the dimer gradually forms from the partial oxidation of DHA and decomposes and, consequently, both the conversion efficiency and the recovery efficiency are diminished.

#### Regeneration cutoff voltage effect

Another critical factor that may impact the effectiveness of regeneration is the cutoff voltage of the regeneration step itself. Figure 2a shows that the dimer oxidation is initiated at a cell voltage of around 0.0 V. However, it is crucial to determine the minimum cutoff voltage at which dimer oxidation completes but the other species present in the negolyte remain unchanged. Unnecessarily lowering the regeneration cutoff voltage, which causes a higher oxidative potential for the negolyte, leads to the possibility of oxygen evolution reaction<sup>18</sup>, and also the oxidation of the carbonaceous electrode itself<sup>19</sup>. More importantly, very oxidative voltages may also result in the decomposition of the electroactive species, DHAQ in our case. As presented in Figure S5, applying a very negative voltage (-0.4 V) to a DHAQ | Ferrocyanide cell led to forming side products in the negolyte not present in a pristine DHAQ electrolyte.

Figures 3a and b show the dependency of the conversion efficiency on regeneration cutoff voltage and the highest potential that the negolyte experiences. The experiments were performed using chemically synthesized DHA instead of oxidizing the DHA that gradually forms through cycling of DHAQ. Not only does this approach shorten the length of experiments, but it also decreases the uncertainty in the results.

According to Figure 3a, the conversion of DHA to DHAQ is incomplete at a regeneration cutoff voltage of 0.0 V. Whereas a conversion efficiency of almost 80% is achieved in 2.0 M OH<sup>-</sup>, the efficiency in 1.0 M OH<sup>-</sup> is only 65% at 0.0 V regeneration cutoff. Lowering the cutoff voltage to -0.1 V, i.e. reverse-polarizing the cell, raises the conversion efficiency. The dependence of the conversion efficiency on cutoff voltage is more intense in 1.0 M OH<sup>-</sup>. This figure corroborates the implication from Figure 2b that some amount of dimer decomposition is inevitable and a conversion of 100% does not seem attainable. Figure 3a also shows that lowering the cell regeneration cutoff voltage below -0.1 V does not improve the conversion efficiency. As shown in Figure S5, applying a very negative cell voltage (-0.4 V) may lead to the formation of undesired species.

The cell voltage for the regeneration step should be adjusted accordingly when a posolyte with a different composition is used. Figure 3b shows the conversion efficiency vs. the maximum potential the negolyte experiences at each regeneration cutoff voltage reported in Figure 3a. These values were measured with the help of a reference electrode (RE) as described in the SI (Figure S7). According to Figure 3b, the conversion efficiency approaches a maximum when the negolyte experiences an oxidation potential of around 0.45 V (vs. SHE) beyond which the conversion efficiency remains essentially unchanged.

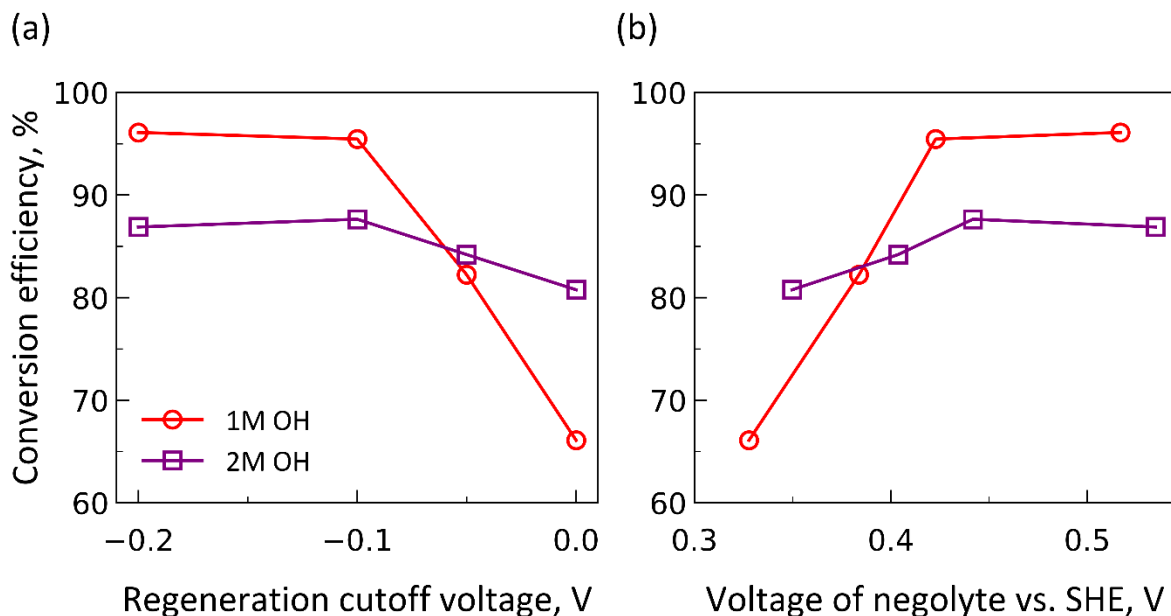


Figure 3: Conversion efficiency of DHA to DHAQ as a function of a) cell regeneration cutoff voltage and b) maximum oxidation voltage (vs. SHE) that the negolyte experiences during the regeneration step. Test conditions: negolyte contained 6.5-7.0 ml of 0.05 M DHA and the posolyte comprised 120 ml of 0.04 M potassium ferrocyanide and 0.02 M potassium ferricyanide. DHA oxidation condition: constant current density at 2 mA/cm<sup>2</sup> followed by potentiostatic hold until a cutoff current density of 0.75 mA/cm<sup>2</sup>. Subsequent cycling of the formed DHAQ was performed under constant current density at 50 mA/cm<sup>2</sup> followed by a potentiostatic hold. The cutoff voltage for the charge and discharge steps were 1.4V and 1.0 V, respectively. Cutoff current densities for the charge and discharge steps were 2 mA/cm<sup>2</sup>.

For the results reported in Figure 3, the electrochemical oxidations were performed under a constant-current (CC) step followed by a constant-voltage (CV) step to exclude the impact of cell internal resistance changes on the extent of the reaction completion<sup>20</sup>. The CC step was usually set at a current density of 2 mA/cm<sup>2</sup> to force a slow oxidation reaction for both DHA and the dimer. To explore whether the oxidation rate affects the conversion efficiency, oxidation was performed an order of magnitude more rapidly at a current density of 20 mA/cm<sup>2</sup>. With such a change, in 2.0 M OH<sup>-</sup> and a cutoff voltage of -0.1 V, the conversion efficiency remained almost unchanged. However, at a cutoff voltage of -0.2 V, the conversion efficiency decreased to 84% at 20 mA/cm<sup>2</sup> from 89% at 2 mA/cm<sup>2</sup>. Although this variation is quite small, such a decline may further confirm the adverse effect of a very low cutoff voltage on the conversion of DHA to DHAQ.

This observation, which seems consistent with the slight decline in the conversion shown in Figure 3 in 2 M OH<sup>-</sup> at cutoff voltages lower than -0.1 V, may be explained as follows. Under slow DHA/dimer oxidation, most of the reaction occurs in the CC region at a voltage above the cutoff value; see, e.g., Figure 2a. At a faster DHA/dimer oxidation rate, however, the cell voltage quickly approaches the cutoff voltage. If the main electroactive species, DHAQ in this case, is unstable at very low cell voltages as indicated by Figure S5, then more DHAQ may decompose when the cell spends longer at lower voltages during the faster oxidation rate. Although the cutoff voltage for the results shown in Figure S5 is -0.4V, DHAQ may decompose to a lesser extent at cutoff voltages explored in Figure 3. We interpret these results to mean that the rate of oxidation of DHA does not adversely affect the conversion efficiency as long as the cutoff voltage is not harmful to the main reactive species. This safe cutoff cell voltage appears to be closer to -

0.1 V, i.e. a negolyte voltage of 0.45 V vs. SHE. Thus, the conversion of DHA to DHAQ can be performed faster only if the cutoff voltage is chosen properly.

#### Period of electrochemical regeneration events

It is crucial to determine how the period of performing the regeneration events impacts the recovery efficiency. Period is defined as the amount of time between the initiation of successive regeneration steps. We hypothesized that the effect of the period is linked to the DHA concentration accumulated in the electrolyte. To investigate this issue, two sets of experiments were performed.

For the first set, the conversion of DHA to DHAQ was measured at different initial concentrations of DHA. The oxidation of DHA and cycling of the formed DHAQ were performed under conditions similar to those described in Figure 3. In 2.0 M OH<sup>-</sup>, when the DHA initial concentration is reduced from 50 mM to 2.5 mM, the conversion efficiency changes only from 88% to 85%. This change, however, is not significant because of the uncertainties involved in measuring transferred charges in the experiment. Therefore, the conversion efficiency appears to be essentially independent of the DHA concentration present in the electrolyte.

The second set of experiments was performed using cells initially containing DHAQ in which DHA formed and accumulated gradually during cycling from the DHAQ<sup>4-</sup> disproportionation. In this set of tests, the period between regeneration events was varied. The recovery efficiencies are reported in Figure 4.

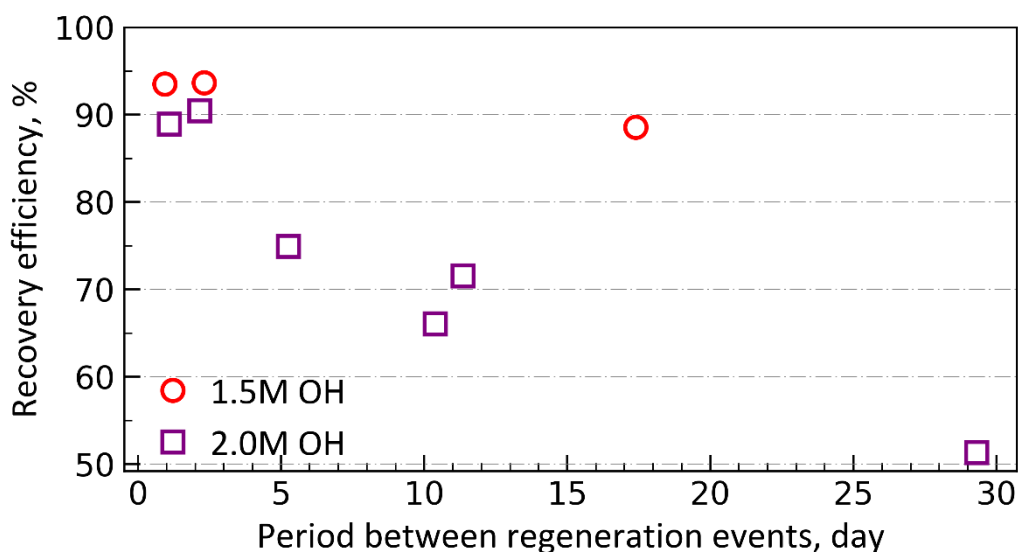


Figure 4: Recovery efficiency vs. period between regeneration events. Test conditions: negolyte comprised 7.0 ml (10 ml for the test in 1.5 M OH<sup>-</sup>) of 0.1 M DHAQ and the posolyte comprised 120 ml of 0.06 M potassium ferrocyanide and 0.03 M potassium ferricyanide. Cell cycling was performed under a constant current density of 50 mA/cm<sup>2</sup> followed by a potentiostatic hold. The cutoff voltage for the charge and discharge steps were 1.4 V and 1.0 V, respectively. Cutoff current densities for the charge and discharge steps were 2 mA/cm<sup>2</sup>. Regeneration steps were performed under a constant current density of 10 mA/cm<sup>2</sup> followed by potentiostatic hold at - 0.15 V until a cutoff current density of 0.75 mA/cm<sup>2</sup> was reached.

As shown in Figure 4, the recovery efficiency declines significantly when the period between regeneration events increases. For these experiments, cells were cycled with a discharge cutoff voltage of 0.95 V or higher, which is high enough to prevent the formation of the unstable dimer until the

regeneration step is initiated. In 2.0 M OH<sup>-</sup>, whereas the recovery efficiency is over 88% when the regeneration step is performed every one or two days, it drops significantly with increasing period. The same trend is observed for 1.5 M OH<sup>-</sup>; however, the extent of decline is noticeably lower.

Thus, Figure 4 clearly shows that regeneration should be performed frequently to retain a high recovery efficiency over the long term. This may, however, increase the risk of unbalancing the cell. The risk is that the oxygen evolution reaction (OER) may also proceed at the negative electrode during the regeneration step. Given that the OER consumes OH<sup>-</sup>, the pH of the negolyte gradually declines and, consequently, the fade rate of the cell is accelerated (Figure 1b). Nevertheless, if the regeneration cutoff voltage is chosen properly (Figure 3), the extent of OER can be reduced. Alternatively, after the regeneration step, oxygen (air) can be introduced into the negolyte to counteract the imbalance. This approach, however, requires measuring the pH of both the posolyte and negolyte to prevent over-exposure of oxygen.

#### Electrochemical regeneration plus SOC restriction

After realizing the importance of the operating conditions as discussed above, experiments were designed to determine the minimum achievable fade rate for a DHAQ | ferrocyanide/ferricyanide cell. Cycling tests were performed at OH<sup>-</sup> concentrations of 1.0, 1.5, and 2.0 M. SOC restriction and regeneration techniques were integrated into cell cycling and operating conditions, such as cutoff voltage of the discharge and regeneration steps, were chosen properly to obtain the lowest fade rate at each of the OH<sup>-</sup> concentrations. The results are presented in Figure 5.

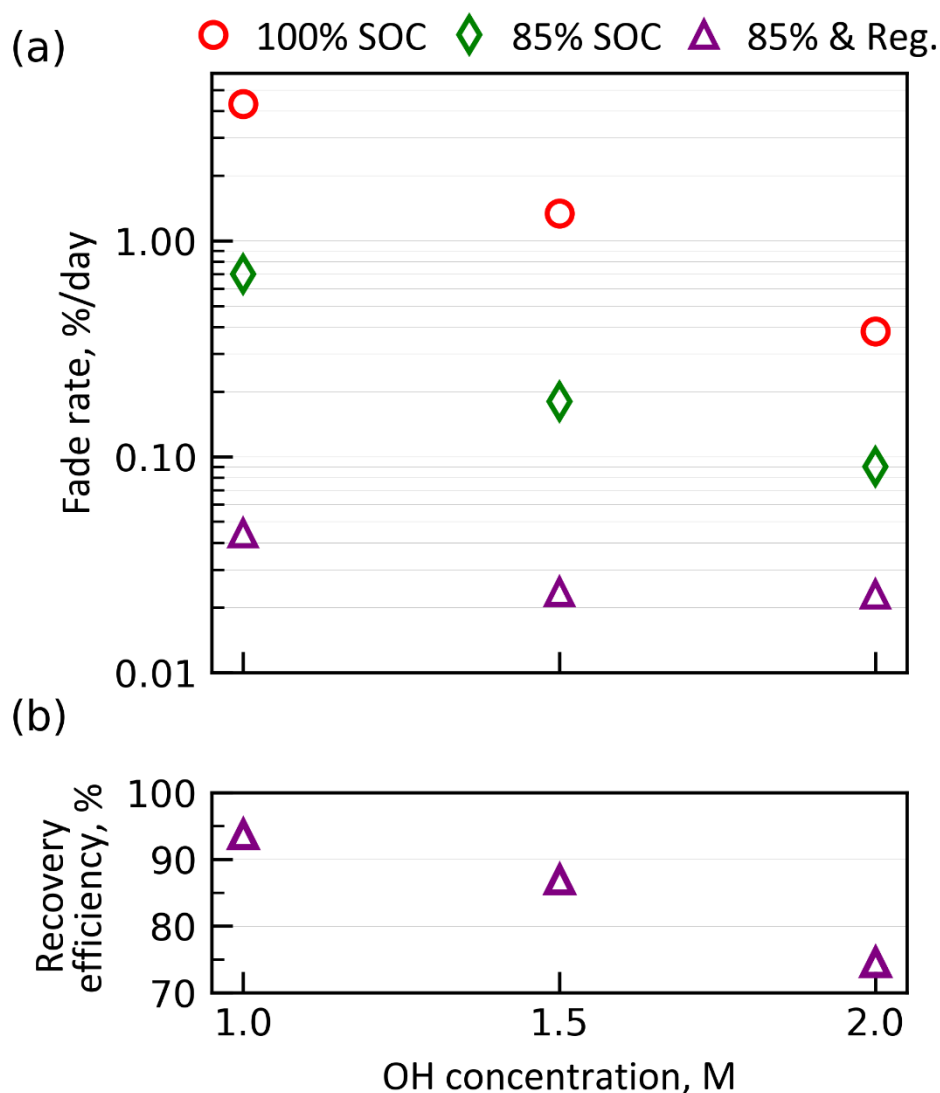


Figure 5 a) Fade rate vs. OH<sup>-</sup> concentration under the following conditions: 100% cycling, 0-85% SOC cycling, and 0-85% SOC cycling combined with regeneration. b) Recovery efficiency vs. OH<sup>-</sup> concentration for the cycling case when 0-85% SOC and the regeneration step are combined. The tests were run for an extended amount of time; the sequence of 0-85% SOC cycling followed by a regeneration step was repeated at least 6 times. Recovery efficiency and fade rates are the averages over the entire test (see SI and Figure S1 for more details). Test conditions: negolyte comprised 7.0 (or 10 ml for the test in 1.5 M OH<sup>-</sup>) of 0.1 M DHAQ and the posolyte comprised 120 ml of 0.06 M potassium ferrocyanide and 0.03 M potassium ferricyanide. Cell cycling was performed under a constant current density at 50 mA/cm<sup>2</sup> followed by a potentiostatic hold. The cutoff voltage for the charge and discharge steps were 1.4 V and 1.0 V, respectively. Cutoff current densities for the charge and discharge steps were 2 and 1 mA/cm<sup>2</sup>, respectively. For 0-85% SOC restriction step, charging capacity was controlled not to exceed 85% of the total capacity of the cell. Regeneration steps were performed under a constant current density at 10 mA/cm<sup>2</sup> followed by potentiostatic hold at -0.15 V until a cutoff current density of 0.75 mA/cm<sup>2</sup> was reached.

Figure 5a shows the fade rate versus OH<sup>-</sup> concentration under different cycling conditions including 100%, 0-85% SOC restriction, and 0-85% SOC restriction combined with a regeneration step; the values at 100% cycling are copied from Figure 1 for comparison purposes. The impact of SOC restriction on the fade

rate of a DHAQ flow cell was previously reported in 1 M OH<sup>-</sup> <sup>14</sup>. However, Figure 5a shows how a combination of SOC restriction cycling and OH<sup>-</sup> concentration affects the fade rate. Under 0-85% SOC cycling conditions, as the OH<sup>-</sup> concentration increases to 2.0 M, the fade rate decreases to 0.09%/day. Thus, with a combination of 85% SOC restriction and OH<sup>-</sup> concentration, a fade rate of 0.09%/day is achievable that is ~8 and ~45 times lower than the fade rate in 1 M OH<sup>-</sup> with and without employing 0-85% SOC restriction, respectively. This observation confirms that increasing the OH<sup>-</sup> concentration beyond 1.0 M significantly reduces the fade rate even when the SOC restriction technique is utilized.

Figure 5a also shows the fade rate for the case when 0-85% SOC restriction and the regeneration are both integrated into the cell cycling. The measured fade rate in 1.0 M OH<sup>-</sup> is around 0.05%/day (18.3%/year) but it decreases to 0.02%/day (7.3%/year) in 1.5 M OH<sup>-</sup>. Nonetheless, the fade rate remains unchanged when OH<sup>-</sup> concentration is further increased to 2.0 M. Therefore, there is no benefit to the fade rate by increasing the OH<sup>-</sup> concentration beyond 1.5 M when both SOC restriction and regeneration are implemented. This observation is related to a lower recovery efficiency. As shown in Figure 5b, the recovery efficiency decreases to 74% in 2.0 M OH<sup>-</sup>. Although the lowest fade rate is obtained in 2M OH<sup>-</sup> under both 100% cycling and 0-85% cycling conditions, the fade rate in the presence of the regeneration is not lowered because the recovery efficiency is the lowest in 2.0 M OH<sup>-</sup>.

Due to performing regeneration step, a loss in energy efficiency is anticipated. Nevertheless, this loss is negligible and remains lower than 0.5% as shown in Figure S6. Therefore, the energy cost of regeneration is not a critical factor in determining the period between regeneration events.

The minimum fade rate of 0.02%/day demonstrated in this study is the lowest ever reported for a DHAQ | ferrocyanide/ferricyanide flow cell. At such a low fade rate, given its low estimated cost of manufacture, DHAQ may now become a viable negolyte for some energy storage applications.

## Conclusions

In this study we explore the dependency of capacity fade rate of a flow battery utilizing 2,6-dihydroxyanthraquinone (DHAQ) as the negolyte on conditions including hydroxide concentration, state of charge (SOC) limits, cutoff voltage of the discharge step, cutoff voltage for electrochemical regeneration by oxidation of decomposition compounds back to active species, and periodicity of performing electrochemical regeneration.

Our experiments confirm that increasing the OH<sup>-</sup> concentrations from 1.0 to 1.5 and 2.0 M decreases the fade rate from 4.3%/day to 1.34 and 0.38%/day, respectively. Under 0-85% SOC restriction conditions, the fade rate at those OH<sup>-</sup> concentrations reach 0.7, 0.18, and 0.09%/day, respectively. Clearly, combining 0-85% SOC cycling with a higher OH<sup>-</sup> concentrations greatly decreases the fade rate. Additionally, with the effect of the regeneration technique, the fade rate is observed to be around 0.05 and 0.02%/day, in 1.0 and 1.5 M OH<sup>-</sup>, respectively. The fade rate in 2.0 M OH<sup>-</sup> is also 0.02%/day, which is not lower than that in 1.5 M OH<sup>-</sup> because of a lower recovery efficiency. The recovery efficiency drops from 94% to 87% and to 74% as the OH<sup>-</sup> concentration increases from 1.0 to 1.5 and 2.0 M.

The recovery efficiency also depends on the periodicity of performing the regeneration technique. To achieve higher recovery efficiencies, it seems essential to perform the regeneration step very frequently. Given a higher fade rate in 1M OH<sup>-</sup>, a more frequent regeneration step is needed. The associated loss in energy efficiency remains lower than 0.5%.

Employing the recommendations and choosing proper cycling conditions for DHAQ enables us to achieve a fade rate as low as 0.02%/day. This fade rate is 18 times lower than the lowest rate reported previously of 0.38%/day, and over 200 times lower than the value under standard cycling conditions of 4.5%/day. We interpret the results with a picture in which the first decomposition product, 2,6-dihydroxyanthrone, is stable but after electro-oxidative dimerization, the anthrone dimer decomposes. We identify conditions for which there is little time after dimerization until the dimer is rapidly re-oxidized electrochemically to form 2,6-dihydroxyanthraquinone. The findings and their mechanistic interpretation are expected to extend the lifetime and enhance the effectiveness of *in-situ* electrochemical regeneration for other electroactive species with finite lifetimes. Here we list recommendations for controlling the fade rate of anthraquinone-based flow cells with a finite lifetime.

- Increasing the OH<sup>-</sup> concentration above 1.0 M significantly reduces the fade rate.
- The discharge cutoff voltage should be adjusted such that the formation of DHA dimer, which is unstable chemically, is eliminated until when the regeneration step is initiated.
- Combining SOC restriction and regeneration techniques is very effective in further reducing the fade rate.
- Choosing a proper cutoff voltage for the regeneration step is critical to maximize recovery efficiency while preventing the decomposition of electroactive species.
- The period between the start of successive regeneration events is another important factor affecting the recovery efficiency. Because the energy cost of regeneration is quite negligible, a low period between regeneration events is recommended.

## Acknowledgements

Research was supported by US DOE award no. DE-AC05-76RL01830 through PNNL subcontract no. 535264, and by a grant from the Massachusetts Clean Energy Center. The funders had no role in study design, data collection and analysis, decision to publish or preparation of the manuscript. We thank Eric M. Fell, Eliza K. Spear, and Dr. Kiana Amini for useful discussions.

## Conflicts of interest

M.B., M.J.A., and R.G.G. have ownership stakes in Quino Energy, Inc., which may profit from the results reported herein.

## References:

- (1) Rugolo, J.; Aziz, M. J. Electricity storage for intermittent renewable sources. *Energ Environ Sci* **2012**, *5* (5), 7151-7160. DOI: 10.1039/c2ee02542f.
- (2) Kittner, N.; Lill, F.; Kammen, D. M. Energy storage deployment and innovation for the clean energy transition. *Nat Energy* **2017**, *2* (9). DOI: 10.1038/nenergy.2017.125.
- (3) Skyllas-Kazacos, M.; Chakrabarti, M. H.; Hajimolana, S. A.; Mjalli, F. S.; Saleem, M. Progress in Flow Battery Research and Development. *J Electrochem Soc* **2011**, *158* (8), R55-R79. DOI: 10.1149/1.3599565.
- (4) Bahari, M.; Watt, G. D.; Harb, J. N. An Asymmetric Viologen-Based Negolyte with a Low Redox Potential for Neutral Aqueous Redox Flow Batteries. *J Electrochem Soc* **2021**, *168* (9), 090525. DOI: 10.1149/1945-7111/ac21f4.
- (5) Beh, E. S.; De Porcellinis, D.; Gracia, R. L.; Xia, K. T.; Gordon, R. G.; Aziz, M. J. A Neutral pH Aqueous Organic-Organometallic Redox Flow Battery with Extremely High Capacity Retention. *ACS Energy Letters* **2017**, *2* (3), 639-644. DOI: 10.1021/acseenergylett.7b00019.
- (6) Ji, Y.; Goulet, M. A.; Pollack, D. A.; Kwabi, D. G.; Jin, S.; Porcellinis, D.; Kerr, E. F.; Gordon, R. G.; Aziz, M. J. A Phosphonate-Functionalized Quinone Redox Flow Battery at Near-Neutral pH with Record Capacity Retention Rate. *Advanced Energy Materials* **2019**, *9* (12), 1900039. DOI: 10.1002/aenm.201900039.
- (7) Jin, S.; Fell, E. M.; Vina-Lopez, L.; Jing, Y.; Michalak, P. W.; Gordon, R. G.; Aziz, M. J. Near Neutral pH Redox Flow Battery with Low Permeability and Long-Lifetime Phosphonated Viologen Active Species. *Advanced Energy Materials* **2020**, *10* (20), 2000100. DOI: 10.1002/aenm.202000100.
- (8) Huskinson, B. T.; Marshak, M. P.; Suh, C.; Er, S.; Gerhardt, M. R.; Galvin, C. J.; Chen, X.; Aspuru-Guzik, A.; Gordon, R. G.; Aziz, M. J. A metal-free organic-inorganic aqueous flow battery. *Nature* **2014**, *505* (7482), 195-198. DOI: 10.1038/nature12909.
- (9) Jing, Y.; Fell, E. M.; Wu, M.; Jin, S.; Ji, Y.; Pollack, D. A.; Tang, Z.; Ding, D.; Bahari, M.; Goulet, M.-A.; et al. Anthraquinone Flow Battery Reactants with Nonhydrolyzable Water-Solubilizing Chains Introduced via a Generic Cross-Coupling Method. *Acs Energy Lett* **2021**, *7* (1), 226-235. DOI: 10.1021/acsenergylett.1c02504.
- (10) Wu, M.; Bahari, M.; Fell, E.; Gordon, R. G.; Aziz, M. J. High-Performance Anthraquinone with Potentially Low Cost for Aqueous Redox Flow Batteries. *Journal of Materials Chemistry A* **2021**, *9*, 26709-26716. DOI: 10.1039/d1ta08900e.
- (11) Wu, M.; Bahari, M.; Jing, Y.; Amini, K.; Fell, E. M.; George, T. Y.; Gordon, R. G.; Aziz, M. J. Highly Stable Low Redox Potential Quinone for Aqueous Flow Batteries. *Batteries & Supercaps* **2022**, e202200009. DOI: 10.1002/batt.202200009.

- (12) Lin, K.; Chen, Q.; Gerhardt, M. R.; Tong, L.; Kim, S. B.; Eisenach, L.; Valle, A. W.; Hardee, D.; Gordon, R. G.; Aziz, M. J.; Marshak, M. P. Alkaline quinone flow battery. *Science* **2015**, *349* (6255), 1529-1532, 10.1126/science.aab3033. DOI: 10.1126/science.aab3033.
- (13) Gregory, T. D.; Perry, M. L.; Albertus, P. Cost and price projections of synthetic active materials for redox flow batteries. *Journal of Power Sources* **2021**, *499*. DOI: 10.1016/j.jpowsour.2021.229965.
- (14) Goulet, M. A.; Tong, L.; Pollack, D. A.; Tabor, D. P.; Odom, S. A.; Aspuru-Guzik, A.; Kwan, E. E.; Gordon, R. G.; Aziz, M. J. Extending the Lifetime of Organic Flow Batteries via Redox State Management. *J Am Chem Soc* **2019**, *141* (20), 8014-8019. DOI: 10.1021/jacs.8b13295.
- (15) Zhao, E. W.; Liu, T.; Jonsson, E.; Lee, J.; Temprano, I.; Jethwa, R. B.; Wang, A.; Smith, H.; Carretero-Gonzalez, J.; Song, Q.; Grey, C. P. In situ NMR metrology reveals reaction mechanisms in redox flow batteries. *Nature* **2020**. DOI: 10.1038/s41586-020-2081-7.
- (16) Jing, Y.; Zhao, E. W.; Goulet, M. A.; Bahari, M.; Fell, E. M.; Jin, S.; Davoodi, A.; Jonsson, E.; Wu, M.; Grey, C. P.; et al. In situ electrochemical recomposition of decomposed redox-active species in aqueous organic flow batteries. *Nat Chem* **2022**, *14* (10), 1103-1109. DOI: 10.1038/s41557-022-00967-4.
- (17) Wu, M.; Jing, Y.; Wong, A. A.; Fell, E. M.; Jin, S.; Tang, Z.; Gordon, R. G.; Aziz, M. J. Extremely stable anthraquinone negolytes synthesized from common precursors. *Chem* **2020**, *6*, 11. DOI: 10.1016/j.chempr. 2020.03.021.
- (18) Dizaji, M. T.; Li, W. Higher Voltage Redox Flow Batteries with Hybrid Acid and Base Electrolytes. *Engineered Science* **2020**, *11*, 54-65. DOI: 10.30919/es8d1118.
- (19) Möller, S.; Barwe, S.; Masa, J.; Wintrich, D.; Seisel, S.; Baltruschat, H.; Schuhmann, W. Online monitoring of electrochemical carbon corrosion in alkaline electrolytes by differential electrochemical mass spectrometry. *Angewandte Chemie International Edition* **2020**, *59* (4), 1585-1589. DOI: 10.1002/anie.201909475.
- (20) Goulet, M.-A.; Aziz, M. J. Flow battery molecular reactant stability determined by symmetric cell cycling methods. *J Electrochem Soc* **2018**, *165* (7), A1466-A1477. DOI: 10.1149/2.0891807jes.